Organic & Biomolecular Chemistry

RSC Publishing

COMMUNICATION

View Article Online
View Journal | View Issue

Pillar[5]arenes with an introverted amino group: a hydrogen bonding tuning effect†

Cite this: *Org. Biomol. Chem.*, 2013, **11**, 248

Received 19th October 2012,
Accepted 7th November 2012

DOI: 10.1039/c2ob27044g

www.rsc.org/obc

Lei Chen, Zhiming Li, Zhenxia Chen and Jun-Li Hou*

Pillar[5]arenes with introverted amino groups were produced through aminolysis. X-ray analysis demonstrated that the intramolecular hydrogen bonding induced the amino group toward the inner space of the cavity. The kinetic studies and molecular modelings revealed that the hydrogen bonding also contributed to the acceleration of the aminolysis through stabilizing the intermediate.

Introverted synthetic cavities, such as Rebek's introverted cavitands,[1] feature inwardly directed functional groups that are regarded as exclusive attributes of proteins and displayed properties of selective recognition,[2] trapping reactive intermediates[3] and efficient catalysis.[4] Pillar[5]arene represents a new kind of synthetic cavity that exhibits pillar conformation.[5] The substituents on the pillararene point to two opposite directions, which may lead to the formation of longer unique tubular cavities.[6] These cavities are open at both ends[7] and thus different from the self-assembled molecular capsules, cages and cavitands.[8] The unique tubular structures have been demonstrated to be novel useful supramolecular hosts[9] and applied in the construction of new supramolecular polymers,[10] molecular devices,[11] artificial transmembrane channels,[12] as well as chemical and physical responding materials.[13] At the current stage, the functionalization of pillar[5]arene usually occurred at either or both sides of the macrocycle. Arranging a functional group inward of pillar[5]arene might generate a new kind of functional group introverted cavity. Herein, we report the first synthesis of pillar[5]arenes that bear an introverted amino group through accelerated aminolysis, which was tuned by intramolecular hydrogen bonding.

We recently reported that the intramolecular hydrogen bondings between the side-chains on pillar[5]arene could induce the formation of tubular structures.[12a] These hydrogen bondings might also be used to locate functional groups inwardly. To achieve this, the mono-activated ester functionalized pillar[5]arene **1** was prepared from **2**[12b] (Scheme 1). The possibility for the formation of introverted pillar[5]arene (IP) through the aminolysis of **1** was investigated by employing α,ω-alkyldiamine (DA-*n*, *n*: carbon number) and alkylmonoamine (MA-*n*) as substrates (Scheme 2a).

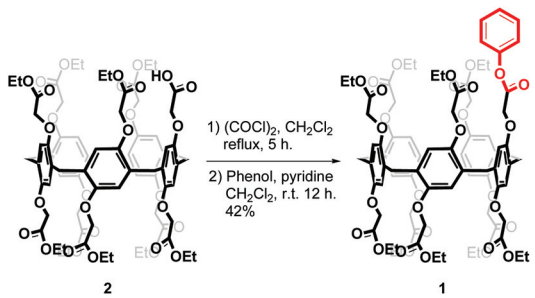

Scheme 1

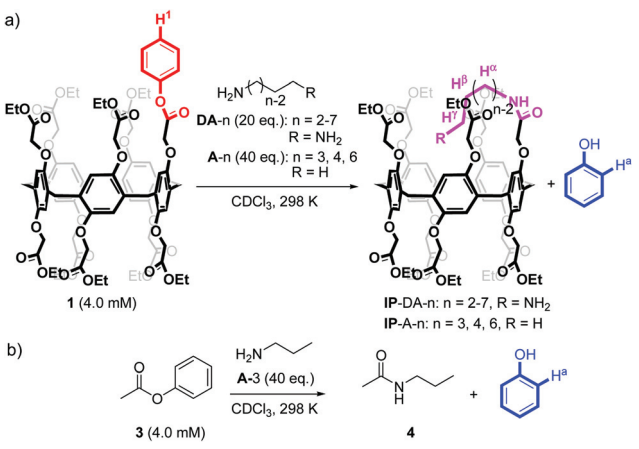

Scheme 2

Department of Chemistry, Fudan University, Shanghai, 200433, P.R. China. E-mail: houjl@fudan.edu.cn; Fax: +86 21 65643712; Tel: +86 21 65105744

†Electronic supplementary information (ESI) available: Synthetic procedures and characterization data, data for kinetic studies, 2D COSY and NOESY ^{1}H NMR specta of IP-A-3, X-ray crystal structure for IP-DA-3 (CIF file). CCDC 903417. For ESI and crystallographic data in CIF or other electronic format see DOI: 10.1039/c2ob27044g

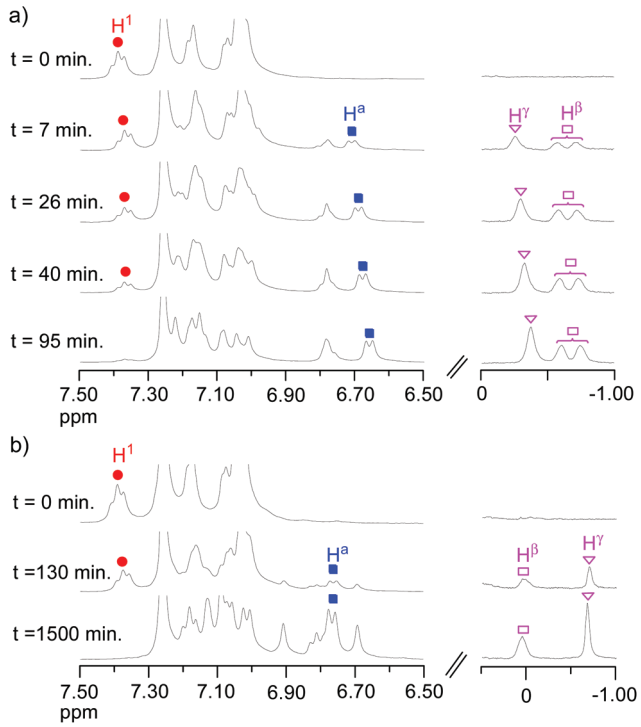

Fig. 1 Partial ^{1}H NMR spectra showing the reaction of **1** (4.0 mM) with (a) DA-3 (80 mM) and (b) MA-3 (160 mM) in $CDCl_3$ at 298 K.

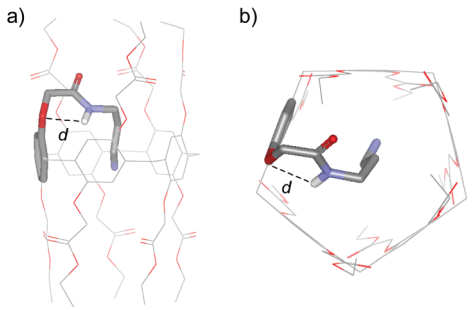

Fig. 2 X-ray crystal structure of IP-DA-3. (a) Side view; (b) top view. The moiety including the hydrogen bonded amide group is highlighted with a stick model. The hydrogen atoms except the one on the amide nitrogen atom are omitted for clarity. d = 2.39 Å.

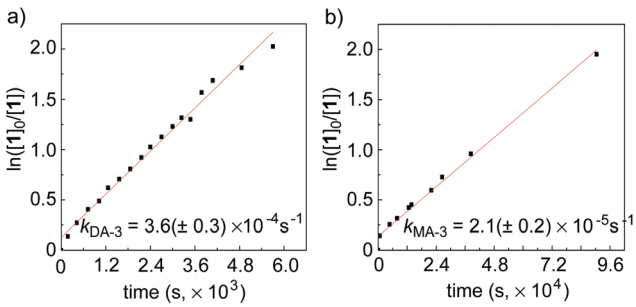

Fig. 3 Kinetic measurements for the reaction of **1** with (a) DA-3 and (b) MA-3. $[\mathbf{1}]_0$ is the initial concentration of **1** (= 4.0 mM); [**1**] is the concentration of **1** at time t. The solid line represents linear simulation of measured data points, of that the slope is the reaction rate constants (k).

The aminolysis of **1** with DA-3 and MA-3 was monitored by using *in situ* ^{1}H NMR experiments (Fig. 1). Mixing the phenol ester **1** (4.0 mM) and DA-3 (80 mM) in deuterated chloroform ($CDCl_3$) at 298 K resulted in the reaction proceeding smoothly, as revealed by the resonance intensity of H^1 on **1** decreasing and H^a on phenol increasing (Fig. 1a). Furthermore, in the upfield area, two sets of new signals were exhibited in the range of 0–1.0 ppm, which were assigned to H^β and H^γ and shifted upfield gradually with the reaction proceeding. The reaction was complete over the course of 95 min. The formation of IP-DA-3 in the mixture was verified by high-resolution ESI-MS (HR ESI-MS) and by comparing the ^{1}H NMR spectrum of the final reaction mixture with the authentic sample (see ESI, Fig. S4†). X-ray crystal structure analysis‡ of IP-DA-3 showed that the amide bond formed intramolecular hydrogen bonding with the adjacent oxygen atoms and the γ-aminopropyl group introverted toward the center of the pillar [5]arene cavity (Fig. 2). Under the strong shielding effect of the tubular cyclophane, the ^{1}H NMR signals of H^β and H^γ shifted upfield. In acetone-d_6, a competitive solvent for the formation of hydrogen bonding, the signals of H^β and H^γ in the range of 0–1.0 ppm were absent from the ^{1}H NMR spectrum, indicating that hydrogen bonding is the main force for keeping the stability of the introverted structure.

The reaction of **1** and MA-3 in $CDCl_3$ at the same concentration and temperature was much slower than the reaction of **1** with DA-3 (Scheme 2a). The reaction was complete over the course of 1500 min to produce IP-MA-3 which was also verified by HR ESI-MS and the authentic sample (Fig. 1b and ESI, Fig. S7†). The propyl group of IP-MA-3 was also introverted as indicated by its upfield shifted H^β and H^γ signals and the NOEs signals of H^β and H^γ with Ar-*H* (see ESI, Fig. S10 and S11†). The reaction of **3** with A-3 under the same conditions was fairly slow and was complete only after ten days (Scheme 2b). For the three reactions, the amino substrates were in large excess. Thus, it is reasonable to assume that the reactions were of pseudo-first order, which was also verified by the linear plots of $\ln([\mathbf{1}]_0/[\mathbf{1}])$ or $\ln([\mathbf{3}]_0/[\mathbf{3}])$ against time (Fig. 3 and ESI, Fig. S13–22†). The reaction rate constants (k), the slope of the linear plots, for the reactions of **1** + DA-3, **1** + MA-3 and **3** + MA-3 were calculated to be 3.6 (±0.3) × 10^{-4}, 2.1 (±0.2) × 10^{-5} and 2.8 (±0.2) × 10^{-6} s^{-1}, respectively.

The rate constants for the reactions of **1** with different DA-*n*s and A-*n*s were also measured and the results are shown in Table 1. For the reactions of DA-*n* (n = 2–7), the values of k varied apparently with the different chain length of DA-*n*, and DA-4 showed the highest rate constants of 4.4 (±0.1) × 10^{-4} s^{-1}, corresponding to a half-life-time ($t_{1/2}$) of 26 min, which indicates a quick reaction. However, for the reaction of A-*n*, the chain length has little influence on the reaction rate. The fact that $k_{\mathbf{1}+\text{DA-}n} > k_{\mathbf{1}+\text{MA-}n} > k_{\mathbf{3}+\text{MA-}n}$ indicates that aminolysis of **1** could be dramatically accelerated by the reaction with DA-*n* and A-*n*. Similar to the introverted alkyl groups of IP-DA-3 and IP-MA-3, the alkyl groups of all the other products of the

Table 1 The reaction rate constants (k) and half-life-times ($t_{1/2}$) of the reactions between **1** or **3** and different amino derivatives[a]

Run	Substrates[b]	k (s^{-1})	$t_{1/2}$
1	**1** + DA-2	$6.4\ (\pm0.3) \times 10^{-5}$	3 h
2	**1** + DA-3	$3.6\ (\pm0.3) \times 10^{-4}$	32 min
3	**1** + DA-4	$4.4\ (\pm0.1) \times 10^{-4}$	26 min
4	**1** + DA-5	$4.3\ (\pm0.2) \times 10^{-5}$	4 h
5	**1** + DA-6	$2.5\ (\pm0.1) \times 10^{-5}$	8 h
6	**1** + DA-7	$2.1\ (\pm0.3) \times 10^{-5}$	9 h
7	**1** + MA-3	$2.1\ (\pm0.2) \times 10^{-5}$	9 h
8	**1** + MA-4	$1.8\ (\pm0.2) \times 10^{-5}$	10 h
9	**1** + MA-6	$1.5\ (\pm0.3) \times 10^{-5}$	12 h
10	**3** + MA-3	$2.8\ (\pm0.2) \times 10^{-6}$	3 d

[a] The reactions were run in $CDCl_3$ at 298 K. [b] [**1**] = [**3**] = 4.0 mM; [DA-n] = 80 mM; [MA-n] = 160 mM.

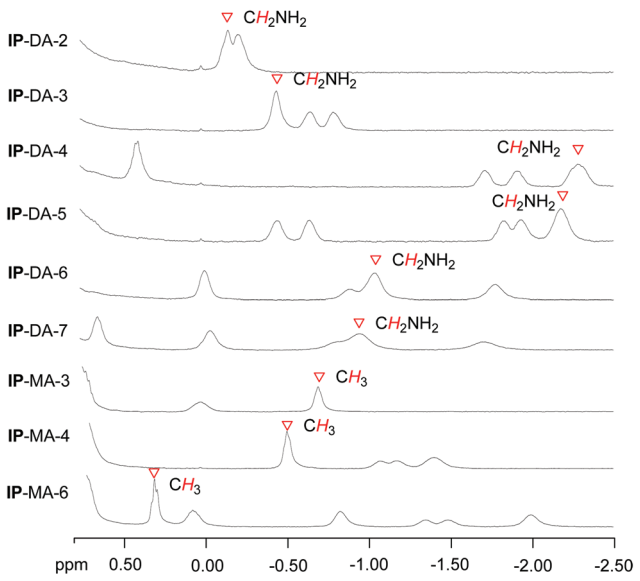

Fig. 4 Partial ^{1}H NMR spectra of IP-DA-n (n = 2–7) and IP-MA-n (n = 3, 4, 6) highlighted the proton signals of introverted side chains. The assignment of the proton signals of CH_2NH_2 and CH_3 based on their integration and non-anisotropic properties.

IP-DA-n and IP-MA-n series are introverted as indicated by their upfield shifted ^{1}H NMR signals in the range of 0–2.5 ppm (Fig. 4). Among the series of IP-DA-n, the signal of CH_2NH_2 of IP-DA-4 showed the largest upfield shifting compared to the chemical shift of CH_2NH_2 in DA-4, indicating that IP-DA-4 might be the one in which the CH_2 connecting to the terminal amino group is closest to the center of the cavity. The position of the amino group in the cavity could be adjusted by using DA-ns of different length as substrates. The values for chemical shift change of CH_3 on the introverted side-chain of IP-MA-n were much smaller than that of CH_2NH_2 on IP-DA-n due to the fast flipping of the side-chain in and out of the cavity (Fig. 4). The fast flipping led to the integration of the introverted side-chain being lower than expected. The reason why the introverted structure of IP-DA-n is more stable than IP-MA-n might be the contribution of hydrogen bonding

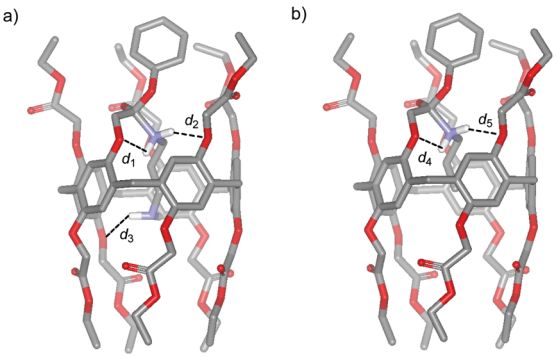

Fig. 5 Geometry optimized structures (hyperchem, semi-empirical, AM1) of aminolysis intermediate (a) $T^{\perp}$(DA-3) and (b) $T^{\perp}$(MA-3). d_1 = 2.29 Å; d_2 = 2.22 Å; d_3 = 2.85 Å; d_4 = 2.37 Å; d_5 = 2.31 Å.

formed between the amino group and the adjacent oxygen atoms.

It is generally recognized that the aminolysis of the phenol ester involves a zwitterionic tetrahedral intermediate ($T^{\perp}$) and the expulsion of phenol is the rate-determining step.[14] To further explore the driving force for the acceleration of aminolysis, molecular modeling on the tetrahedral intermediate of the reaction of **1** with DA-3 and MA-3 was carried out and the results are shown in Fig. 5. For both $T^{\perp}$s, the N–Hs close to the zwitterions were found to form hydrogen bonding with the adjacent oxygen atoms, which stabilize the intermediate and thus the aminolysis was accelerated compared to the reaction of **2** with A-3. On $T^{\perp}$(DA-3), an additional hydrogen bonding formed between the primary amino group and the oxygen atom on the pillar[5]arene backbone. This hydrogen bonding caused $T^{\perp}$(DA-3) to be more stable than $T^{\perp}$(MA-3) and thus $k_{DA\text{-}3}$ is larger than $k_{MA\text{-}3}$. The tendency for formation of hydrogen bonding by the primary amino group on $T^{\perp}$(DA-n) decreased with the increase of the chain length of DA-n. As a result, the k values varied in a large range for the reaction of the DA-n series. In conclusion, we have reported the synthesis of amino group introverted pillar[5]arene which was tuned by intramolecular hydrogen bonding. The hydrogen bonding not only stabilized the introverted structure, but also accelerated the aminolysis through stabilizing the intermediate of the reaction. It is envisioned that the chiral space will be generated by using chiral alkylamines as substrates, which was under investigation.

This work was supported by NSFC (20902012 and 91027008), Program for Changjiang Scholars and Innovative Research Team in University (IRT1117), STCSM (09ZR1402700, 10PJ1401200).

Notes and references

‡Crystallographic data of IP-DA-3 (CCDC 903417): $C_{76}H_{94}N_2O_{29}\cdot(CHCl_3)$, M_r = 1618.93, monoclinic, space group $P2(1)/n$, a = 18.958 (4), b = 21.804 (5), c = 20.210 (5) Å; α = 90, β = 91.004 (4), γ = 90°; V = 8353 (3) Å^3; Z = 4, λ = 0.71073 Å; T = 296 (2) K; 39 475 reflections collected, 14 656 unique reflections (R_{int} = 0.1029); R_1 = 0.1409, wR_2 = 0.3690 [$I > 2\sigma(I)$]; R_1 = 0.2456, wR_2 = 0.4131 (all data).

1 R. J. Hooley and J. Rebek Jr., *Chem. Biol.*, 2009, **16**, 255–264.
2 B. W. Purse and J. Rebek Jr., *Proc. Natl. Acad. Sci. U. S. A.*, 2005, **102**, 10777–10782.
3 T. Iwasawa, R. J. Hooley and J. Rebek Jr., *Science*, 2007, **317**, 493–496.
4 S. R. Shenoy, F. R. Pinacho Crisostomo, T. Iwasawa and J. Rebek Jr., *J. Am. Chem. Soc.*, 2008, **130**, 5658–5659.
5 (*a*) T. Ogoshi, S. Kanai, S. Fujinami, T.-a. Yamagishi and Y. Nakamoto, *J. Am. Chem. Soc.*, 2008, **130**, 5022–5023; (*b*) M. Xue, Y. Yang, X. Chi, Z. Zhang and F. Huang, *Acc. Chem. Res.*, 2012, **45**, 1294–1308; (*c*) P. J. Cragg and K. Sharma, *Chem. Soc. Rev.*, 2012, **41**, 597–607.
6 W. Si, X.-B. Hu, X.-H. Liu, R.-H. Fan, Z. Chen, L. Weng and J.-L. Hou, *Tetrahedron Lett.*, 2011, **52**, 2484–2487.
7 X.-B. Hu, L. Chen, W. Si, Y. Yu and J.-L. Hou, *Chem. Commun.*, 2011, 4694–4696.
8 J. W. Steed and P. A. Gale, *Supramolecular Chemistry: From Molecules to Nanomaterials*, Wiley, 2012.
9 (*a*) C. Han, G. Yu, B. Zheng and F. Huang, *Org. Lett.*, 2012, **14**, 1712–1715; (*b*) G. Yu, C. Han, Z. Zhang, J. Chen, X. Yan, B. Zhen, S. Liu and F. Huang, *J. Am. Chem. Soc.*, 2012, **134**, 8711–8717; (*c*) Y. Ma, X. Chi, X. Yan, J. Liu, Y. Yao, W. Chen, F. Huang and J.-L. Hou, *Org. Lett.*, 2012, **14**, 1532–1535; (*d*) T. Ogoshi, R. Shiga and T.-a. Yamagishi, *J. Am. Chem. Soc.*, 2012, **134**, 4577–4580; (*e*) X. Shu, S. Chen, J. Li, Z. Chen, L. Weng, X. Jia and C. Li, *Chem. Commun.*, 2012, 2967–2969; (*f*) C. Li, K. Han, J. Li, H. Zhang, J. Ma, X. Shu, Z. Chen, L. Weng and X. Jia, *Org. Lett.*, 2012, **14**, 42–45; (*g*) Y. Ma, X. Ji, F. Xiang, X. Chi, C. Han, J. He, Z. Abliz, W. Chen and F. Huang, *Chem. Commun.*, 2011, 12340–12342; (*h*) N. L. Strutt, R. S. Forgan, J. M. Spruell, Y. Y. Botros and J. F. Stoddart, *J. Am. Chem. Soc.*, 2011, **133**, 5668–5671; (*i*) Z. Zhang, Y. Luo, B. Xia, C. Han, Y. Yu, X. Chen and F. Huang, *Chem. Commun.*, 2011, 2417–2419.
10 (*a*) X.-Y. Hu, X. Wu, Q. Duan, T. Xiao, C. Lin and L. Wang, *Org. Lett.*, 2012, 4826–4829; (*b*) Y. Guan, M. Ni, X. Hu, T. Xiao, S. Xiong, C. Lin and L. Wang, *Chem. Commun.*, 2012, 8529–8531; (*c*) Z. Zhang, Y. Luo, J. Chen, S. Dong, Y. Yu, Z. Ma and F. Huang, *Angew. Chem., Int. Ed.*, 2011, **50**, 1397–1401.
11 (*a*) Z. Zhang, C. Han, G. Yu and F. Huang, *Chem. Sci.*, 2012, **3**, 3026–3031; (*b*) N. L. Strutt, H. Zhang, M. A. Giesener, J. Lei and J. F. Stoddart, *Chem. Commun.*, 2012, 1647–1649; (*c*) T. Ogoshi, D. Yamafuji, T. Aoki and T.-a. Yamagishi, *J. Org. Chem.*, 2011, **76**, 9497–9503.
12 (*a*) X.-B. Hu, Z. Chen, G. Tang, J.-L. Hou and Z.-T. Li, *J. Am. Chem. Soc.*, 2012, **134**, 8384–8387; (*b*) W. Si, L. Chen, X.-B. Hu, G. Tang, Z. Chen, J.-L. Hou and Z.-T. Li, *Angew. Chem., Int. Ed.*, 2011, **50**, 12564–12568.
13 (*a*) G. Yu, M. Xue, Z. Zhang, J. Li, C. Han and F. Huang, *J. Am. Chem. Soc.*, 2012, **134**, 13248–13251; (*b*) Y. Yao, M. Xue, X. Chi, Y. Ma, J. He, Z. Abliz and F. Huang, *Chem. Commun.*, 2012, 6505–6507; (*c*) I. Nierengarten, S. Guerra, M. Holler, J.-F. Nierengarten and R. Deschenaux, *Chem. Commun.*, 2012, 8072–8074; (*d*) H. Zhang, N. L. Strutt, R. S. Stoll, H. Li, Z. Zhu and J. F. Stoddart, *Chem. Commun.*, 2011, 11420–11422.
14 (*a*) F. M. Menger and J. H. Smith, *J. Am. Chem. Soc.*, 1972, **94**, 3824; (*b*) A. C. Satterthwait and W. P. Jencks, *J. Am. Chem. Soc.*, 1974, **96**, 7018.